On the way to a pressure tolerant LiDAR for deep sea robot navigation

Group A2

S. Rutten (4472659), D. Looman (4573269),
B. van Vliet (4594959) and D.O. Wijnberg (4578376)

***Abstract*— This paper contributes to advancing the field of underwater navigation by taking a first step towards developing a fluid-filled pressure tolerant LiDAR scanner. A prototype was designed and built to investigate the effects of exposure to a high pressure environment, flow induced optical disturbances and viscous drag losses. This prototype was experimentally verified and the approach promises to be usable in subsea object avoidance applications, as the first of its kind.**

I. Introduction

One of the greatest challenges in subsea robotics remains underwater positioning. Particularly deep sea robots, where teleoperation is often not feasible, require means to avoid obstacles and navigate some trajectory. An LiDAR is a time of flight based laser scanning method used to capture spatial information. LiDAR is increasingly popular for accurate positioning of both terrestrial and aerial autonomous systems. However, according to Massot-Campos and Oliver-Cordina (2015), LiDAR is still rarely used for underwater applications.[1]

Filisetti et al (2019) indicate that only three subsea LiDAR systems are currently commercially available. Besides their slow scan rates, leaving them unsuitable for navigation on moving robots, they also rely on bulky pressure rated housings to protect the internal components from the hydrostatic pressure. Filisetti (2019) states that "significant cost can be attributed to the pressure rated housings for these systems", expanded on further by Teague (2018). The costs of the current systems are in the order of hundreds thousands of dollars and thus accessible to only a niche industry, likely the reason for the limited use of LiDAR in underwater sensing.[2][3]

Bingham (2013) explains that instead of housing a system in a pressure rated casing, the system itself can be designed to be pressure tolerant. This can be accomplished by adapting all compressible elements in the system by either replacing gas pockets with a liquid or by encapsulation using a casting compound. [4] When it comes to optical systems, Kampmann et al (2012) as well as Gelze and Lehr (2011) have demonstrated that miniature pressure tolerant cameras are technically feasible. [5] [6] However, no other publications on pressure tolerant optical systems exist. Even more so, this novel design approach is unexplored in general, even though it has potential for significant cost reduction compared to conventional deep sea systems.

This study investigates whether a fluid-filled, pressure tolerant LiDAR system is technically feasible. Three problems come to mind:

- The increased drag of moving components in the working fluid, compared to in air.
- Thermal management in a fluid-filled system
- The exposure of components to the working fluid.

Three more problems were found in literature;

- The exposure of components to pressure. [7]
- The effect of pressure-dependent variation of the refractive index of fluids. [6]
- The optical disturbances caused by fluid flow in the system. [8] [9] [10]

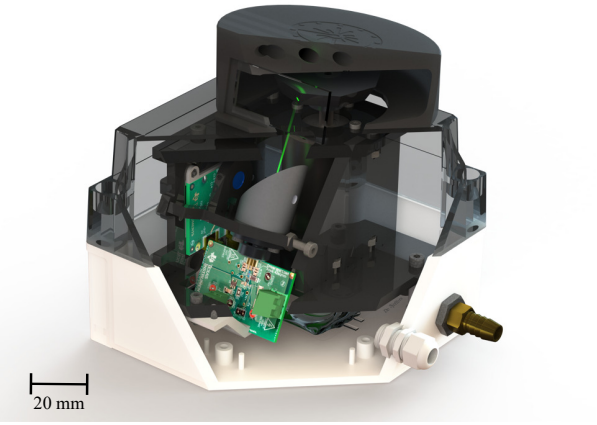

Fig. 1: A cross sectional render of the prototype

The complex nature of these phenomena has led to the choice to build a prototype to test for the aforementioned problems.[1] The resulting prototype (Figure 1) measures 130 mm x 130 mm x 150 mm and weighs 3.6 kg
when filled with fluid. The prototype is designed to have a rectangular field of view of 70° by 30°.

First the design of the prototype is described in section II, along with the conducted tests. The corresponding results (section III) are discussed in section IV and concluded in section V.

II. Methods and Materials

Solutions found to the problems stated in the introduction are combined into a prototype. An overview of these solutions is presented in Figure 2.

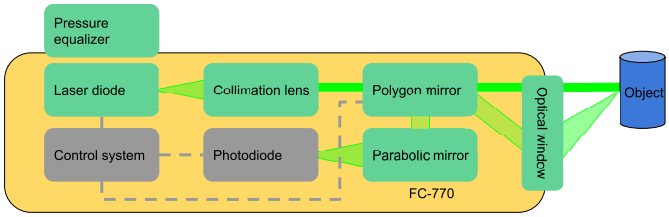

Fig. 2: Functional system diagram

A green laser diode provides a light source.[2] The diode

[1]The control electronics for a time of flight, nanosecond pulsed, type system were developed simultaneously along with the discussed prototype but are beyond the scope of this paper

[2]Conventional LiDAR scanners predominantly use infrared laser light, but due to the different spectral absorption of seawater from air, a wavelength of 520 nm is used. [11]

package contains a gas pocket, which would implode under pressure if it was left unmodified. Implosion was prevented by decanning the diode, presented in Figure 3.

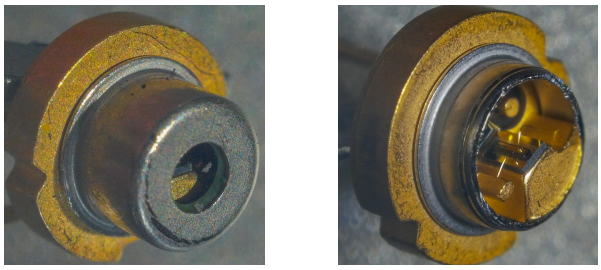

(a) Canned laserdiode (b) Decanned laserdiode

Fig. 3: Decanning was done using a specialized tool

The beam from the laser diode itself is divergent and is therefore collimated by a laser collimating lens, as only the focal distance changes when the surrounding medium has a different index of refraction of air.

The laserbeam is aimed and reflected by the irregular polygon mirror. The polygon mirror allows for 2.5D scanning [3] (see Figure 6) as the eight mirror faces are angled between $20°$ and $35°$, resulting in eight different scan heights over a $30°$ range. Additionally, the use of a polygon allows for constant velocity scanning and reduces energy consumption during operation.

The laser pulse leaves the system trough the window, hits a distant object and is assumed to scatter uniformly in all directions. The fraction of light reflected oriented $180°$ (anti-parallel) to the original laser beam makes it back through the window onto the polygon mirror. The beam is reflected in the same direction as where the laser came from, as the polygon is still in the same position[4]. The returning light is reflected and focused onto the photodiode by the parabolic mirror. As reflections are not affected by the refractive index of the medium, the focal length of a parabolic mirror is thus independent of pressure.

The brushless DC inrunner motor with integrated Hall effect sensors drives the rotating polygon mirror. An absolute magnetic encoder under the motor provides an absolute position reference by tracking the magnetic field direction of a magnet attached to the motor axis and is used to determine the angular velocity. The frame consists of laser cut PMMA sheet. An off the shelf electronics poly-carbonate enclosure, rated IP67, together with a resin printed cover separates the system from seawater. Plastic IP68 cable glands provide external connections.The working fluid is a fluorocarbon named FC-770. [12] This is an electronic coolant and is both chemically and thermally stable, non-toxic, transparent and has a low viscosity. An infusion bag serves as pressure equalizer and compensates for the slight compressibility of the working fluid under pressure and the volume that is lost when any leftover air bubbles shrink under pressure.

In order to verify the proposed solutions of the prototype several tests were conducted.

[3]With 2.5D is meant, a grid of 8 lines resulting in a very high resolution horizontally and a 8 position resolution vertically.

[4]The velocity of the rotating polygon is orders of magnitude lower than the speed of light so it can be reasoned that the rotation of the polygon is negligible during this timespan

Drag losses The relation of the input power and angular velocity was measured both in air and in the working fluid. The angular velocity was increased by increments of 0.5 rev/s every 2 s and both the current and the voltage were measured. The duty cycle was limited to 90% to prevent high currents from harming the motor.

Thermal equilibrium The temperature in the system was measured by inserting a thermocouple into the infusion bag. The motor was turned on for 10 minutes at a velocity of 30 rev/s.

Exposure of components to the working fluid All components were immersed in the working fluid by filling the enclosure. The laser diodes were tested specifically because the protective cover was removed. Three decanned laser diodes were powered with a constant current power supply and the output power was measured using a laser power meter at distance of 10mm. The fourth laser diode was filled with a clear epoxy. Three were submerged in isopropanol, the FC-770 and mineral oil respectively, for five minutes. The diodes were left to drip for a minute and the output of all four were measured again using the method as described. The same three diodes plus the epoxy filled one were then again submerged in their respective fluids for five minutes, this time powered by the constant current supply while submerged. The diodes were left to drip for a minute and the output power was measured.

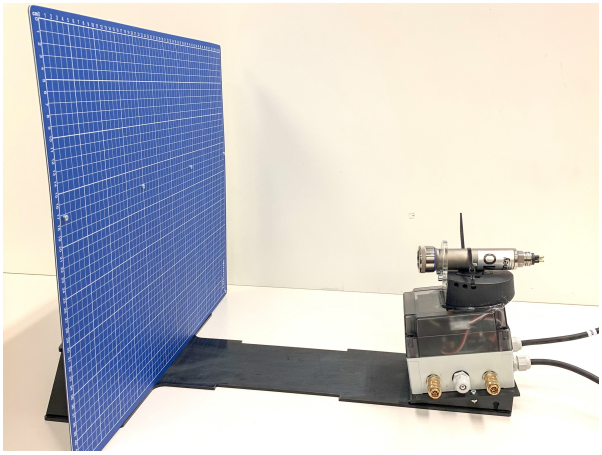

Fig. 4: Image of the test setup and the prototype

For the following tests, an additional test setup was designed and build which can be placed in a pressure chamber, as shown in Figure 4. A raster with a grid size of 10 mm was placed in front of the prototype at fixed distance of 38 cm from the window. A pressure-rated LUXUS compact camera was used to track the laser beam on the raster. The camera returns RGB signal in normal light conditions however, only grey scale signal during low light conditions . The pressure chamber contained a feed through which allowed for motor control, laser control and live video monitoring.

Pressure exposure To confirm the pressure tolerant design the test setup with prototype was tested in a pressure chamber. The pressure in the tank was increased in steps of 20 bar every two minutes up to 100 bar and was thereafter released rapidly back to atmospheric pressure.

Pressure-dependent variation of refractive index During the pressure test, the laser output of the prototype was aimed stationary at the raster. The beam was aimed at around $20°$ to

the left and 5° down from the normal to the window. The laser beam was continuously captured by the camera and was monitored on a screen to capture changes in intensity of the laser spot, focusing of the laser and deflection of the beam. The images were analyzed digitally and the resulting spot sizes measured using the known raster size of 10mm. A baseline test at atmospheric pressure was done. Afterwards,the same test was done at atmospheric pressure and compared to the baseline test.

Flow induced optical disturbances Under atmospheric pressure, both the laser and the motor were powered to project the laser output on the raster and sweep across it. The scan pattern was monitored and filmed using a smartphone from behind the prototype.

III. Results

A functional prototype was designed and realized within the limited time available.

Figure 5 presents the relationship between the power usage of the motor and the angular velocity in FC-770.

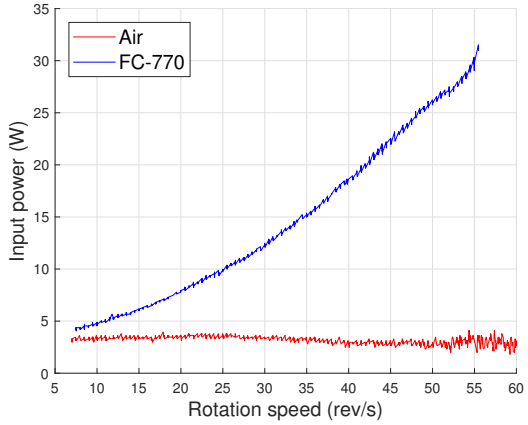

Fig. 5: Power usage of motor plotted against angular velocity

The temperature remained constant at 25°C during 10 minutes of operation at 30 rev/s.

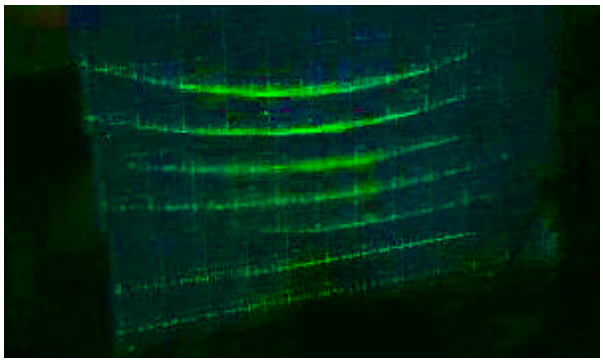

Fig. 6: The scan pattern created by the rotating irregular polygon; the image was enhanced to highlight the scan pattern

Table I shows the output power of the laserdiode pre and post submersion. No other unexpected changes happened when the diodes where submerged. An additional laserdiode was casted in epoxy which performed nominally, it however showed a blurred output. All other components showed no performance loss after submersion in the working fluid.

All components survived pressures up to a 100 bar and the rapid decompression and performed nominally post testing. The off the shelf enclosure together with the resin 3D printed cover and standard cable glands did not leak.

Figure 7 shows the laser output of the prototype under different pressures. There seems to be a negative correlation between the light intensity and pressure and the light intensity seems to be restored when the pressure was released again. At a pressure of 0 bar, the spot diameter is at 5.0 ± 0.5 mm. At 100 bar, the spot diameter has decreased to 3.5 ± 0.5 mm. The position of the spot did not noticeably change relative to the raster.

Figure 6 presents the scan pattern projected on the raster by the prototype. Left over air bubbles from filling were broken up into a mixed flow at atmospheric pressure.

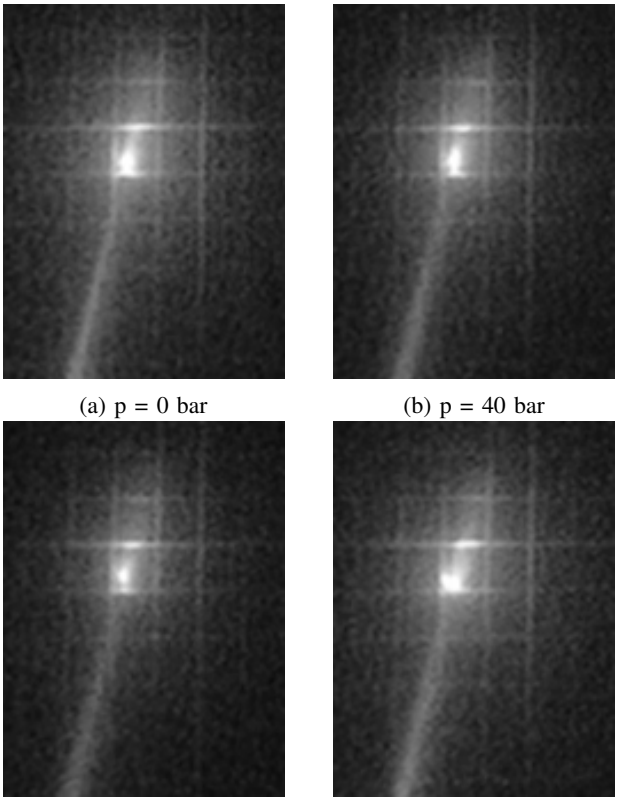

(a) p = 0 bar (b) p = 40 bar

(c) p = 100 bar (d) Released to p = 0 bar

Fig. 7: Laser output under different pressures

TABLE I: Light intensity of decanned laserdiodes in different working fluids

Working fluid	Isopropanol	Mineral oil	FC-770
Decanned	-	0.17 mW	0.22 mW
Post passive test	90 μW	0.00 mW	0.22 mW
Post active test	23 μW	18 μW	0.17 mW
15 min post active test	36 μW	22 μW	0.22 mW

IV. Discussion

The technical feasibility of a pressure tolerant LiDAR system was investigated. Firstly, all components of the prototype survived a pressure of 100 bar, so the application of the pressure tolerant design method has no immediate impediments.

Figure 5 confirms that the motor uses considerably more power in the working fluid compared to operation in air and shows a exponential relation between power and angular velocity. The power consumption of the motor seen in the

figure is 12 W at 30 rev/s is not a technically limiting factor though.

The power consumption of the motor does not result in an increase in temperature of the prototype. A one-dimensional steady-state heat conduction calculation yields an expected temperature rise of 2°C, in line with the obtained results. Even when the control electronics are included in the calculation, the equilibrium temperature is expected to stay within manageable bounds.

As FC-770 is designed for chemical inertness, no compatibility issues were encountered with the prototype. To research the necessity of the package (can), the laserdiode was tested in multiple possible working fluids and the output power has decreased significantly after submerging in isopropanol and mineral oil, and the output of the epoxy casted diode was blurred. So only the decanned laserdiode seems compatible with FC-770.

Figure 7 reveals that the output power of the laser diode has decreased significantly with increased pressure. Dybala et al (2002) show wavelength shift in semiconductor laser sources with the application of high pressure. [13] The camera used to observe the laser while in the pressure chamber could be less sensitive to this different wavelength. However, basic calculations using the data from Dybala et al (2002) show that the wavelength shift is in the order of single nanometers, suggesting that the loss of light intensity observed by the camera can not be attributed to wavelength shift. It may be that the difference between refractive indices of the FC-770 and the semiconductor substrate increases, causing a larger beam divergence. The resulting beam aperture could then be larger than the lens surface, cutting of a portion of the output light. It is difficult to test this hypothesis with the current prototype though.

Concerning the less critical components, off the shelf plastic hardware was demonstrated to be a viable options for constructing deep sea systems. The pressure equalizer consisting of a modified infusion bag also worked as predicted. These extreme low cost solutions remove significant part of the cost of conventional deep sea systems as described by Teague (2018) and Filisetti (2019). [3][2]

The location of the laser spot does not move in the tested pressure range. Possibly, the ratio of refractive index of both the FC-770 and the water in the pressure chamber remains constant, or the changes are too minimal for a visible deflection through the window at this range. The same test setup could be built incorporating mirrors to artificially increase the distance to several meters such that the laser beam travels further, combined with a larger pressure test range, amplifying any deflection. A similar method was employed by Gelze and Lehr (2011). [6]

Weiss et al (2012) show that the refractive index of water increases with higher pressure, implying that FC-770 too has a positive correlation between index of refraction and pressure if the previous hypothesis is assumed true.[14] Unfortunately, not much is known about the pressure dependence of the specific semiconductor of the laser diode, so this hypothesis is of no use to verify whether the change in difference of refractive indices is the cause of the decreased power output of the laser diode under pressure. Further research is needed.

As can be seen in Figure 6, the scanning stage produces clear lines. As the beam is distributed radially, the projection onto a flat plane results in curved lines. The lines are somewhat blurred, likely because of scattering due to the dispersed air bubbles. At higher pressures, the air bubbles will likely disappear along with the scattering, although this should be experimentally verified. Also, more care can be taken during the filling process.

Some aspects have not been tested yet, these include the stability of angular velocity of the polygon, the returning intensity of the laser light as well as the timing electronics for time of flight distance calculation. A complete system test is scheduled for the near future.

V. Conclusion

A first step was made in the development of a fluid-filled pressure tolerant LiDAR. The findings presented in this paper suggest that the pressure-dependent variation of the refractive index, nor the adaptation of standard laser diodes, nor the increased viscous drag poses a significant technical hurdle. This work is the first to demonstrate a fluid-filled laser scanner which can survive high pressures. Together with Kampmann's (2012) findings this contributes to the development a new class of underwater optical sensors enabling cost-effective deep sea robots in support of marine science. The prototype will be further developed for navigation and positioning of underwater robots, as there is no commercial off the shelf solution at this moment.

References

[1] M. Massot-Campos and G. Oliver-Codina, "Optical Sensors and Methods for Underwater 3D Reconstruction." *Sensors (Basel, Switzerland)*, vol. 15, no. 12, pp. 31 525–57, dec 2015. [Online]. Available: http://www.ncbi.nlm.nih.gov/pubmed/26694389

[2] A. Filisetti, A. Marouchos, A. Martini, T. Martin, and S. Collings, "Developments and applications of underwater LiDAR systems in support of marine science," *OCEANS 2018 MTS/IEEE Charleston, OCEAN 2018*, no. January, pp. 1–10, 2019.

[3] J. Teague, M. J. Allen, and T. B. Scott, "The potential of low-cost ROV for use in deep-sea mineral, ore prospecting and monitoring," *Ocean Engineering*, vol. 147, no. November 2017, pp. 333–339, 2018. [Online]. Available: https://doi.org/10.1016/j.oceaneng.2017.10.046

[4] Bingham, "Designing pressure-tolerant electronic systems," Unmanned Underwater Technology, Tech. Rep., 2013.

[5] P. Kampmann, J. Lemburg, H. Hanff, and F. Kirchner, "Hybrid Pressure-Tolerant Electronics," *2012 Oceans*, pp. 1–5, 2012.

[6] J. Gelze and H. Lehr, "On the way to a pressure-tolerant imaging system," *OCEANS'11 MTS/IEEE KONA*, pp. 1–4, 2011.

[7] Bingham, "Pressure tolerant electronics (pte) for deep ocean vehicle applications," 2017, hardware Developers Didactic Galactic. [Online]. Available: https://medium.com/supplyframe-hardware/building-pressure-tolerant-electronics-pte-for-deep-ocean-\vehicle-applications-da42869a5c78

[8] R. J. Hill, "Optical propagation in turbulent water," *Journal of the Optical Society of America*, vol. 68, no. 8, p. 1067, 1978.

[9] G. F. Marshall and G. E. Stutz, *Handbook of Optical and Laser Scanning*. CRC press, 2011, ch. 4, p. 788. [Online]. Available: http://books.google.com/books?id=MLWUatLv0s0C{&}pgis=1

[10] L. Sun, J. Wang, K. Yang, M. Xia, and J. Han, "The Research of Optical Turbulence Model in Underwater Imaging System," *Sensors & Transducers Journal*, vol. 163, no. 1, pp. 107–112, 2014.

[11] P. M. Moser, "Spectral transmission of light through sea water," Pacific-Sierra Research Corporation, Tech. Rep. September, 1992. [Online]. Available: http://www.dtic.mil/docs/citations/AD1012965

[12] *3M Fluorinert Electronic Liquid FC-770 - Product Information*, 3M, 6 2007, rev. 10.0.

[13] F. Dybala, P. Adamiec, A. Bercha, R. Bohdan, and W. Trzeciakowski, "Wavelength tuning of laser diodes using hydrostatic pressure," *Proc. SPIE*, vol. 4989, 06 2003.

[14] L. Weiss, A. Tidu, A. Tazibt, and M. Aillerie, "Optical properties of water under high pressure," 09 2012.